IC/86/136
INTERNATIONAL REPORT
(Limited Distribution)

International Atomic Energy Agency
and
United Nations Educational Scientific and Cultural Organization
INTERNATIONAL CENTRE FOR THEORETICAL PHYSICS

# CALCULATION OF THE UNSTEADY FLOW IN VANELESS DIFFUSERS BY THE PARTIALLY-PARABOLIC METHOD

M. Bassily Hanna *
International Centre for Theoretical Physics, Trieste, Italy.

ABSTRACT

Experimental investigations have shown that the flow discharged from a centrifugal compressor or pump impeller into the diffuser is unsteady and contributes for additional losses in the diffuser. The partially parabolic method is used to calculate this flow in the diffuser and reveals the mechanism of smoothing the distorted flow downstream. Calculated results are compared with measurements and good agreement is found.

MIRAMARE - TRIESTE
July 1986

* Permanent address: Faculty of Engineering and Technology, Minia University, Minia, Egypt.

## Introduction

Many experimental results have shown that a great part of the losses in radial compressors occur in the diffuser, due to the distorted unsteady flow discharged from the radial impeller [1,2]. The classical method for calculating the flow in vaneless diffusers treats the flow as one dimensional, using empirical values for the frictional coefficients [3].
Owing to the great difference between the calculated values using this method and experimental results, in case of the highly unsymmetrical flow, the losses in vaneless diffusers would be treated in two steps, namely :

(a) the unsymmetrical flow will be assumed to be equalized suddenly, so that the losses can be calculated as Carnot losses [3,4],
(b) after the equalization of the flow it can be treated as one dimensional [3].

Another development to treat the unsteady distorted flow in vaneless diffusers was done by Dean and Senoo [1]. The flow is devided into two regions, the so called Jet and Wake regions. Using some assumptions and empirical values for the frictional coefficients, which vary from case to case [5], it is possible to notice the way of the flow equalization and the vanishing of the wake.

In this paper a procedure to calculate the three dimensional flow discharged in a parallel walled vaneless diffuser will be presented. Such flow is regarded as unsteady flow in the absolute system [1]. The flow rotates with the angular velocity of the impeller and due to its nonuniformity the velocity at a certain point in the absolute system varies with the time ( $\partial / \partial t \neq 0$).
The flow will be assumed to be incompressible and turbulent from

the beginning. To overcome the flow unsteadiness in the absolute system, the problem will be treated in a relative system rotating with the angular velocity of the impeller. For this purpose the partially parabolic method will be used [6].

**The Partially Parabolic Procedure**

It is possible to solve the equations of motion as parabolic equations, if the pressure field is known and the tensional stresses will be neglected. That the elliptic effect can be given only through the known pressure distribution. Due to this fact, the diversion of the solution will greatly depend on the accuracy of the starting pressure field [6]. Because it is difficult to give the correct pressure distribution in advance, it is usual to calculate the pressure for starting the procedure assuming isentropical conditions. According to this assumption, the velocity components calculated parabolic will not satisfy the continuity equation. Therefore the pressure field must be iteratively corrected untill the continuity equation is fulfilled for every point of the cross-section under consideration.

**The Coordinate System:** As the flow discharged from the impeller into the diffuser is unsteady, when regarded in the absolute system, the solution will be derived using a cylindrical coordinate system rotating with the impeller angular velocity (Fig. 1).

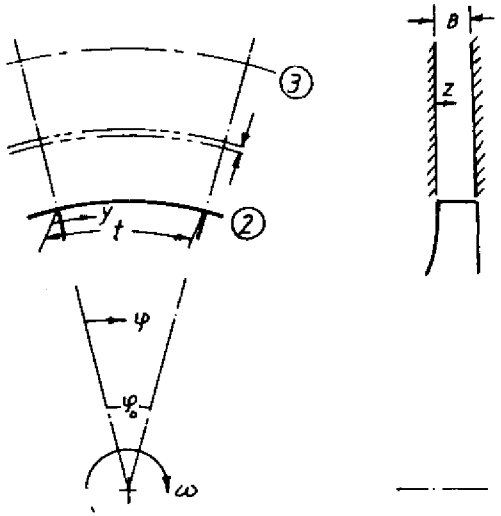


Fig.1 Rotating coordinate system



**Fundamental Equations:** Using the cylindrical coordinates shown in Fig.1, the fundamental equations for incompressible flow can be expressed as follows [7] :

**Continuity equation**

$$\frac{\partial}{\partial r}(r\,w_r) + \frac{\partial w_\varphi}{\partial \varphi} + r\,\frac{\partial w_z}{\partial z} = 0 \qquad (1)$$

**Momentum equations**

Under the assumption, that the flow is turbulent from the beginning and that the tensional stresses and the shear stresses in flow direction are negligible, the momentum equations tend to:

r-direction

$$w_r\frac{\partial w_r}{\partial r} + \frac{w_\varphi}{r}\frac{\partial w_r}{\partial \varphi} + w_z\frac{\partial w_r}{\partial z} - \frac{w_\varphi^2}{r} - 2\omega\,w_\varphi - \omega^2 r = -\frac{1}{\rho}\frac{\partial p}{\partial r} + \frac{1}{\rho}\left(\frac{1}{r^2}\frac{\partial}{\partial \varphi}\left(\mu\frac{\partial w_r}{\partial \varphi}\right) + \frac{\partial}{\partial z}\left(\mu\frac{\partial w_r}{\partial z}\right)\right) \qquad (2a)$$

$\varphi$ -direction

$$w_r\frac{\partial w_\varphi}{\partial r} + \frac{w_\varphi}{r}\frac{\partial w_\varphi}{\partial \varphi} + w_z\frac{\partial w_\varphi}{\partial z} + \frac{w_r\,w_\varphi}{r} + 2\omega\,w_r = -\frac{1}{\rho}\frac{1}{r}\frac{\partial p}{\partial \varphi} + \frac{1}{\rho}\left(\frac{1}{r}\frac{\partial}{\partial z}\left(\mu\frac{\partial w_z}{\partial \varphi}\right) + \frac{\partial}{\partial z}\left(\partial\frac{\partial w_\varphi}{\partial z}\right)\right) \qquad (2b)$$

z-direction

$$w_r\frac{\partial w_z}{\partial r} + \frac{w_\varphi}{r}\frac{\partial w_z}{\partial \varphi} + w_z\frac{\partial w_z}{\partial z} = -\frac{1}{\rho}\frac{\partial p}{\partial z} + \frac{1}{\rho}\left(\frac{1}{r^2}\frac{\partial}{\partial \varphi}\left(\mu\frac{w_z}{\partial \varphi}\right) + \frac{1}{r}\frac{\partial}{\partial \varphi}\left(\mu\frac{\partial w_\varphi}{\partial z}\right)\right) \qquad (2c)$$

where

$$\mu = \mu_l + \mu_t$$

## Turbulence model

The determination of the apparent viscosity in the case of three dimensional distorted shear flow is normally difficult. A simple model based on Prandtl's assumptions will be used here.
Owing to the three dimensional velocity distribution, two values for the apparent viscosity can be calculated (using the velocity gradient either in $\varphi$ -direction or in z-direction). As long as the apparent viscosity determined in z-direction is greater than in $\varphi$-direction, it will be considered as the effective apparent viscosity. Otherwise a mean value of $\mu_{t\varphi}$ and $\mu_{tz}$ will be regarded as the effective apparent viscosity.

$$\mu_t = \begin{cases} \mu_{tz} & \{\mu_{tz} > \mu_{t\varphi}\} \\ (\mu_{tz} + \mu_{t\varphi})/2 & \{\mu_{tz} < \mu_{t\varphi}\} \end{cases} \qquad (3)$$

Depending on the shear flow, the apparent viscosity will be determined in two ways as follows :

### a. Wall boundary layer regions

Near the walls the eddy viscosity will be calculated using Prandtl's mixing-length theory [7]

$$\mu_t = \rho\, l^2 \left( \left( \frac{1}{r} \frac{\partial w_r}{\partial \varphi} \right)^2 + \left( \frac{\partial w_r}{\partial z} \right)^2 + \left( \frac{\partial w_\varphi}{\partial z} + \frac{1}{r} \frac{\partial w_z}{\partial \varphi} \right)^2 \right)^{1/2} \qquad (4)$$

where

$l = 0.41\, z$ (z ≡ distance to the nearest wall)

In the outer range of the boundary layers :

$l = l_{max} = \lambda . \delta$ ( $l < l_{max}$ )

$\lambda = 0.08 - 0.09$

$\delta$ is the boundary layers thickness

### b. Free turbulent flow

The shear flow outside the wall boundary layers will be treated as free turbulent flow (Fig. 2). The virtual kinematic viscosity will be calculated using the simple form established by Prandtl [8] :

$$\mu_t = \rho\, \kappa_1\, b\, (w_{rmax} - w_{rmin}) \qquad (5)$$



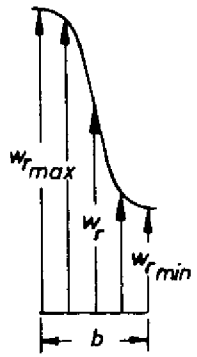


**Fig. 2** Free turbulent flow outside the boundary layers

The constant $\kappa_1$ in equation (5) must be determined on the basis of measured values. Here it will be set equal to $\beta^2$ determined experimentally for the wake behind a cylinder [8]. ( $\beta = 1/b = 0.18$) With this value a good agreement with the measurements is reached. b in Equation (5) is the shear flow width (Fig.2). $w_{rmax}$ and $w_{rmin}$ are the maximum and minimum radial velocities.

## Determination of the static pressure field

According to measurements (e.g. [1],[2]), the pressure fluctuation will be damped in a short distance after a radial impeller. As such a good starting value for the pressure distribution can be obtained from the simple frictionless one dimensional calculation. For parallel-walled vaneless diffusers, the pressure can be expressed as follows [5] :

$$\frac{\bar{p}(r+\Delta r) - \bar{p}(r)}{\rho\, c(r)^2/2} = 1 - \left( \frac{r}{r+\Delta r} \right)^2 \qquad (6)$$

where

$\bar{p}(r)$ and $\bar{p}(r+\Delta r)$ are the pressures acting at the radii r and $r+\Delta r$ respectively. $c(r)$ is the mean velocity acting at r.

## Pressure correction

Using the pressure distribution calculated out from equation (6) and the starting conditions, the velocity components $w_r$ , $w_\varphi$ and $w_z$ can be calculated from equations (2a,b,c) with the aid of a

marching integration technique [6]. This solution will not be completely correct, because of the unexactly calculated pressure field and the calculated components will not satisfy the continuity equation. Accordingly the pressure field must be corrected to give the proper velocity distribution.
The correct values of the pressure and velocity components will be expressed as the sum of the unexactly calculated values (*) and a correction part (') [6] :

$$\begin{aligned} w_r &= w_r^* + w_r' \\ w_\varphi &= w_\varphi^* + w_\varphi' \\ w_z &= w_z^* + w_z' \\ p &= p^* + p' \end{aligned} \qquad (7)$$

The difference between the values calculated by substituting equation (7) in the momentum equation (2a), where the variation in the curvature, shear stresses and Coriolis terms as well as the correction in the transport velocities will be neglected, and those calculated using (*) data, yields for the momentum equation in the radial direction [7] :

$$w_r^* \frac{\partial \grave{w}_r}{\partial r} + \frac{w_\varphi^*}{r} \frac{\partial \grave{w}_r}{\partial \varphi} + w_z^* \frac{\partial \grave{w}_r}{\partial z} = - \frac{1}{\rho} \frac{\partial \grave{p}}{\partial r} \qquad (8)$$

For more simplification it will be assumed that :

$$w_r^* >> w_\varphi^* , w_z^*$$

Then tends equation (8) to :

$$w_r^* \frac{\partial \grave{w}_r}{\partial r} = - \frac{1}{\rho} \frac{\partial \grave{p}}{\partial r} \qquad (9a)$$

In the same way the other two momentum equations in $\varphi$- and z-directions will be treated and the correction in the velocity components can be given as a function of the pressure correction as follows :

$$w_r^* \frac{\partial \grave{w}_\varphi}{\partial r} = - \frac{1}{\rho} \frac{1}{r} \frac{\partial \grave{p}}{\partial \varphi} \qquad (9b)$$

$$w_r^* \frac{\partial \grave{w}_z}{\partial r} = - \frac{1}{\rho} \frac{\partial \grave{p}}{\partial z} \qquad (9c)$$



A first step to correct the pressure over the cross-section under consideration can be obtained from equation (9a), that fulfills the continuity equation finally. Because the pressure for the previous section is already corrected, it can be written :

$$\rho \, \grave{w}_r = - \frac{1}{w_r^*} \grave{p} \qquad (10)$$

Integrating equation (10) over the considered cross-section, tends equation (10) to [7] :

$$\bar{\grave{p}} = \frac{\dot{m} - \dot{m}^*}{\iint_A \frac{1}{w_r^*} r \, d\varphi \, dz} \qquad (11)$$

$\bar{p}'$ corrects the pressure level to satisfy the continuity equation as a whole. The second pressure correction will be done to satisfy the continuity equation in every point of the cross-section. Using the continuity equation together with equations (7), the defect in the continuity (-CD) can be interpreted as follows :

$$\rho \left\{ \frac{\partial}{\partial r} r \grave{w}_r + \frac{\partial \grave{w}_\varphi}{\partial \varphi} + r \frac{\partial \grave{w}_z}{\partial z} \right\} = - \rho \left\{ \frac{\partial}{\partial r} r w_r^* + \frac{\partial w_\varphi^*}{\partial \varphi} + r \frac{\partial w_z^*}{\partial z} \right\} = -CD \qquad (12)$$

The continuity defect (-CD) can be calculated from the first solution of the momentum equations (2). The correction for the velocity components in equation (12) will be expressed as pressure correction using equations (9) :

$$\left( \frac{r}{\Delta r} + 1 \right) \frac{\grave{p}}{w_r^*} + \frac{\partial}{\partial \varphi} \left( \frac{\Delta r}{r} \frac{1}{w_r^*} \frac{\partial \grave{p}}{\partial \varphi} \right) + r \frac{\partial}{\partial z} \left( \frac{\Delta r}{w_r^*} \frac{\partial \grave{p}}{\partial z} \right) = CD \qquad (13a)$$

$$f_1 \, p' + f_{2\varphi} \, p'_\varphi + f_{3z} \, p'_z + f_{2\varphi\varphi} \, p'_{\varphi\varphi} + f_{3zz} \, p'_{zz} = CD \qquad (13)$$

where

$$f_1 = \frac{1}{w_r^*} \left( \frac{r}{\Delta r} + 1 \right) \; ; \; f_2 = \frac{\Delta r}{r} \frac{1}{w_r^*} \; ; \; f_3 = r \frac{\Delta r}{w_r^*}$$

Equation (13) represents the local pressure correction for every point of the cross-section. The numerical solution of this equation is not stable. As a proposal from Moore [6] -1% of f will be considered, which means, that the local pressure level correction will be varied to stabilize the numerical solution. This variation will not affect the gradient of the pressure correction in $\varphi$- and z-direction. The value of $\partial p'/\partial r$ used after that will be multiplied with -0.01 to compensate the difference

in the local pressure correction level. Finally, the pressure correction can be calculated as follows :

$$p^{*}_{new} = p^{*}_{old} + \bar{p}'$$

and then

$$p = p^{*}_{old} + \bar{p}' + p' \qquad (14)$$

(see solution procedure)

It must be mensioned that equation (14) will be used only for the velocity correction. For the pressure correction, the part $p'$ will be added to the one-dimensionally calculated pressure $p^{*}$.

**Boundary conditions**

Because of the adhesion, the absolute velocity must be zero at the diffuser walls. To use this boundary condition, the grid lines at the diffuser walls must be very dense, because of the high velocity gradient in this region, and the sublayer region must be taken into account.
As a simplification, the absolute velocity at the wall (point 0 in Fig. 3) will not be set equal zero, but will be linearly extrapolated from the neighbouring point (point 1 in Fig. 3), assuming the same flow angle for both points. The velocity components in the absolute system can be expressed as functions of those in the rotating system as follows :

$$c_r = w_r$$

$$c_\varphi = w_\varphi + \omega r \qquad (15)$$

$$c_z = w_z$$

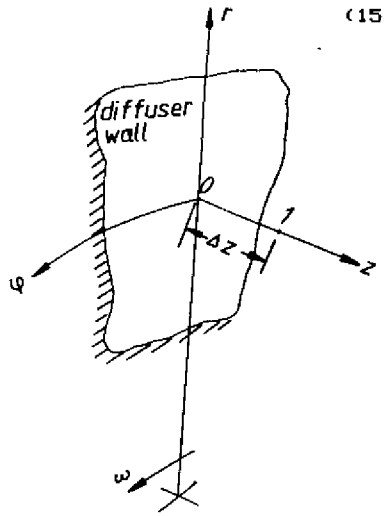


**Fig.3** Coordinate system for determinig the velocity components at the walls



Because point 1 is very near to the wall, the velocity component perpendicular to the wall can be neglected.

$$c_{z1} = c_{z0} = 0 \qquad (16)$$

For determinig the friction velocity $u_\tau$ , the absolute velocity at point 1 must be known. For this purpose the downstream velocity distribution will be used as starting values and after that by the iteration the calculated values for the considered cross-section will be used.

$$c_1 = \sqrt{w_{r1}^2 + ( w_{\varphi 1} + \omega r )^2} \qquad (17)$$

Using Prandtl's velocity-distribution law [9] :

$$c_1 = \frac{u_\tau}{.41}\left( \ln \left( \frac{\Delta z\, u_\tau}{\nu} \right) + 2 \right) \qquad (18)$$

By iteration procedure the friction velocity $u_\tau$ can be determined from equation (18) and then the velocity gradient in z-direction at point 1 :

$$\left( \frac{\partial c}{\partial z} \right)_1 = \frac{u_\tau}{0.41\, \Delta z} \qquad (19)$$

Assuming that the flow angle for point 1 and 0 is the same and using equations (19) and (15), then for linear extrapolation between point 1 and 0 (Fig. 3) it can be written :

$$w_{r0} = w_{r1}\left( 1 - \frac{u_\tau}{0.41\, c_1} \right) \qquad (20a)$$

$$w_{\varphi 0} = ( w_{\varphi 1} + \omega r )\left( 1 - \frac{u_\tau}{0.41\, c_1} \right) - \omega r \qquad (20b)$$

**Solution procedure**

The solution will be carried out on a diffuser sector, representing the flow discharged from an impeller channel. A marching integration technique is used, in which a two-dimensional field of variables is determined with the finite-difference procedure, at each section of the sector considered.
The flow diagram in Fig.4 explains the steps of the solution :

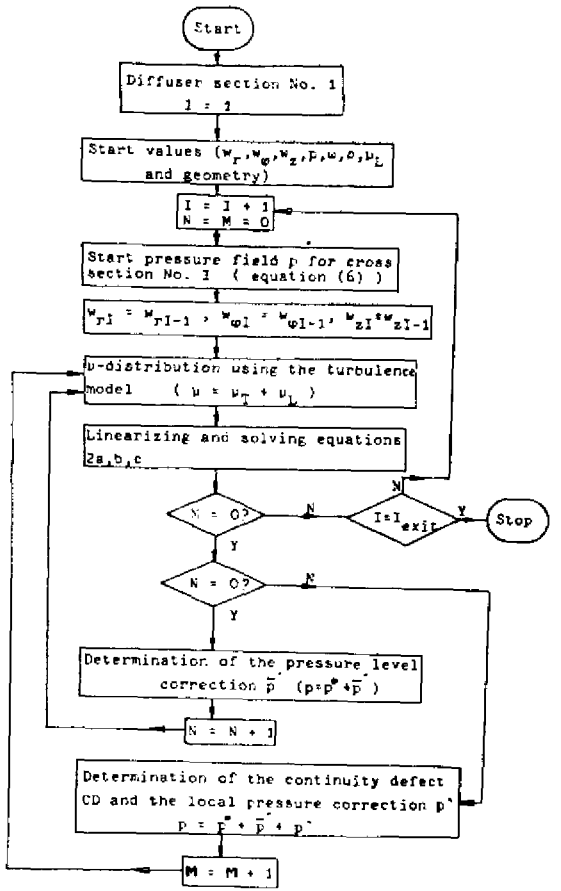


**Fig. 4** Flow diagram for computing the flow in vaneless diffusers



1. The initial values of the flow and the diffuser geometery will be stored for the grid knots shown in Fig. 5.

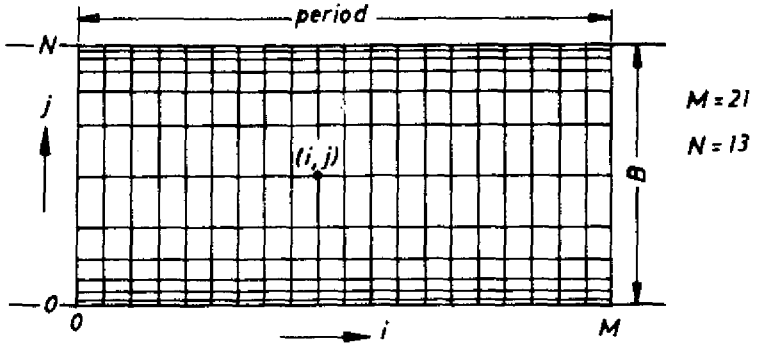


**Fig. 5** Grid used for calculating the flow

2. The pressure for the next section will be calculated one-dimentionally with the help of equation (6).
3. The dynamic viscosity will be detrmined with the aid of the velocity components either from the downstream or, when it is iterated, from the calculated velocity components.
4. The radial velocity distribution $w_r$ will be implicitly calculated after linearizing equation (2a) using, at first, the unknown variables from the previous cross-section.
5. The velocity components $w_\varphi$ and $w_z$ will be determined similarly from equations (2b) and (2c) using the calculated $w_r$ and $w_\varphi$ respectively.
6. The pressure level will be corrected according to eqn. (11).
7. Using the corrected pressure level and the calculated velocity components, the steps 3 till 5 will be repeated, to determine more exact values for the velocity distribution.
8. The defect in the continuity (CD) for every point of the cross-section considered will be determined using eqn. (12). With this value the local pressure correction p' will be calculated from equation (13).
9. Step 3 till 5 will be repeated using the velocity components calculated in point 7 and the corrected pressure distribution in point 8.
10. The values obtained will be stored and will be used as starting values for the next cross-section.
11. Step 2 till 9 will be repeated till the diffuser exit will be reached.

**Results**

The procedure demonstrated in the previous chapters will be applied to calculate the flow discharged in the vaneless diffuser measured by Eckardt [2] to test the validity of this method. The second case is the computation of different kinds of flow with

varying grades of distortion, which will be given in the rotating system in the form of a sine function with different amplitudes. Hypothetical values for the flows will be used in this comparision. The aim is, besides the investigation of the mechanism of equalization of the unsymmetrical flow, a study of the additional losses due to the distortion of the flow.

**a. Eckardt's diffuser**

Eckardt's diffuser (Fig. 6) is a very important object of investigation, because of the two-dimensional character of the velocity field. The operating point m = 5.31 kg/s and N=14000 RPM will be calculated assuming that, the flow is incompressible and the variation of the diffuser width in the regions measured - within radius ratio $R/R_2$ of 1.017 and 1.151 - is negligible.

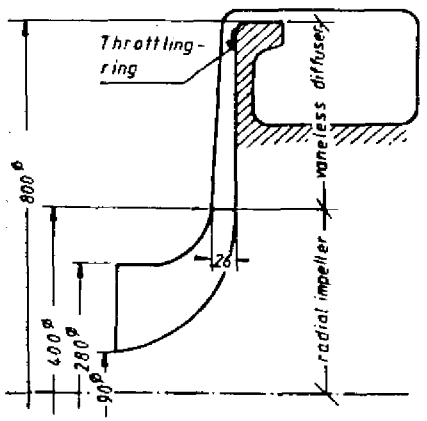


**Fig. 6** Geometry and main dimensions of Eckardt's diffuser

Fig.7 shows the measured and the calculated three dimensional radial velocity distribution along different radii of Eckardt's diffuser. It must be noticed, that Eckardt's measurements are not given in a certain sector representing a period, but always represented between the pressure- and the suction- side. In the calculation, for a constant sector having the same angle as the impeller channel, the pressure and the suction side will be shifted from radius to radius. This shifting, which occurs due to the swirl in flow, can be seen in Fig. 7. The agreement between the calculated and the measured $w_r$ -distributions is good. It can be noticed, that the heavily distorted flow is equalized in a relatively short radial distance.



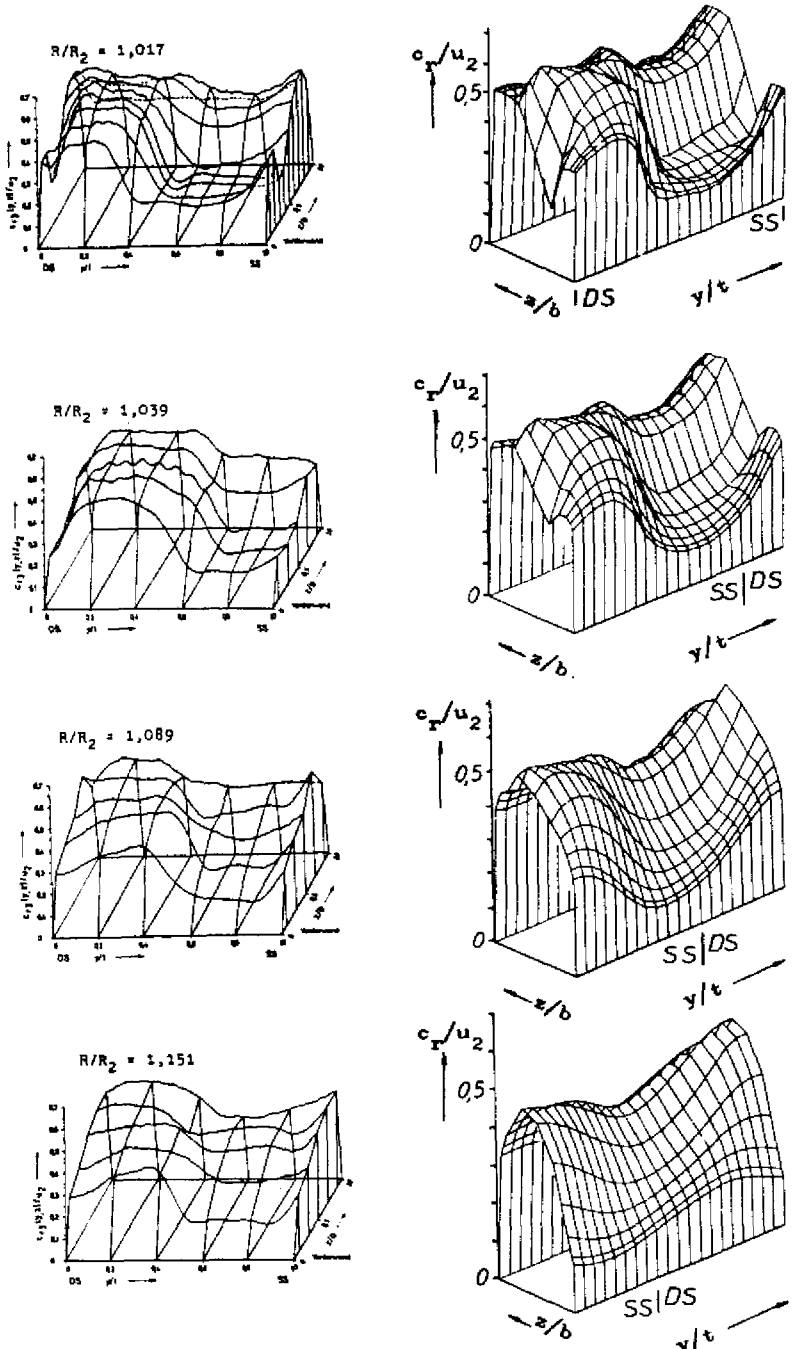


**Fig.7** Measured and calculated radial velocity distribution

Fig. 8 shows the measured values of the total pressure, compared with those calculated using the present procedure and the Dean and Senoo method. The slope of the curve detrmined here is almost the same as that of the measured points ◘ (instantaneously measured points [2]). This is not achieved by Dean and Senoo method in both cases of considering the flow as compressible or incompressible. The difference occured in the level is due to the assumption of incompressibility of the flow. The total pressure $p_t$ in case of incompressible flow is determined according to equation (21) :

$$p_t = p + \varrho c^2/2 \qquad (21)$$

In the case of compressible flow, we must start with the total enthalpy $h_t$, which equals to the sum of the static enthalpy h and the kinetic energy :

$$h_t = h + c^2/2 \qquad (22a)$$

Using the principal equations of the thermodynamics assuming isentropic stagnation process, equation (22a) tends to :

$$p_t = p \left[ 1 + \frac{\gamma - 1}{\gamma} \frac{\varrho}{p} \frac{c^2}{2} \right]^{\frac{\gamma}{\gamma - 1}} \qquad (22)$$

It is clear that the total pressure determined using equation (21) differs from that calculated with the help of equation (22) for the same static pressure and the same kinetic energy. This causes the difference in the level between the curves in Fig.8.

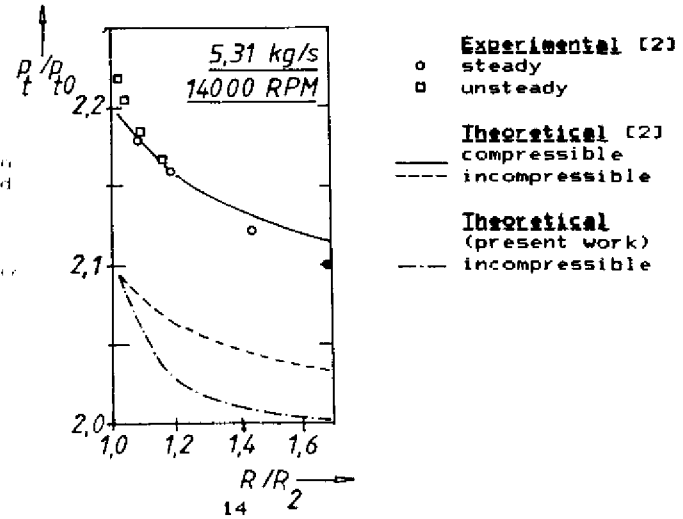


Fig. 8 Comparison between measured and calculated dimensionless total pressure in atmospheric test pressure



For the incompressible flow the difference in the total pressure is proportional to the losses in the diffuser. This is shown in Fig. 9, where a better agreement is reached with the present procedure than that of Dean and Senoo. (Point 2' represents the location of the first diffuser section measured by Eckardt [2])

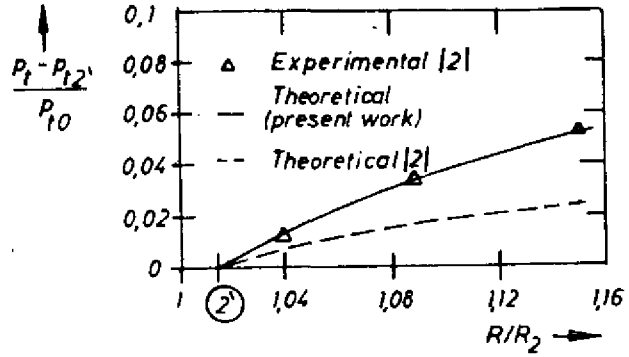


Fig. 9 Total pressure difference at different radii

**b. Effect of the unsymmetry upon the losses**

The geometry of the vaneless diffuser will be taken the same as that of the radial compressor at the "Institut fur Strahlantriebe und Turboarbeitsmaschinen RWTH Aachen, west Germany" (see Fig.10).

$\dot{m} = 0,75$ kg/s

$N = 8000$ RPM

$z = 16$ blades

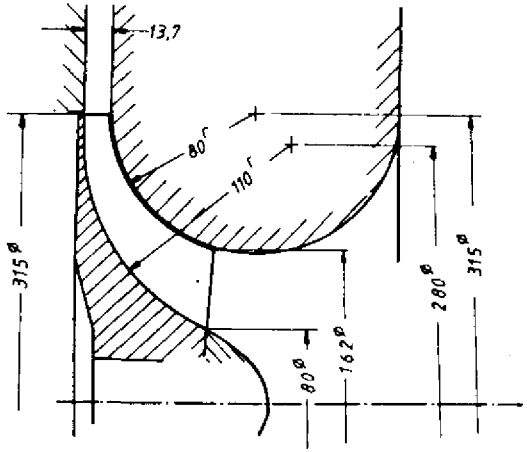


Fig. 10 Geometry and main dimensions of the RWTH radial compressor

Three cases with different grades of distortion will be calculated. The radial velocity distribution in the circumferential direction will be given according to the following equation (Fig. 11) :

$$w_r(\varphi) = w_{rm} [\, 1 + k \sin( z\ \varphi ) \,] \qquad (23)$$

where k is a distortion parameter and z is the number of blades.

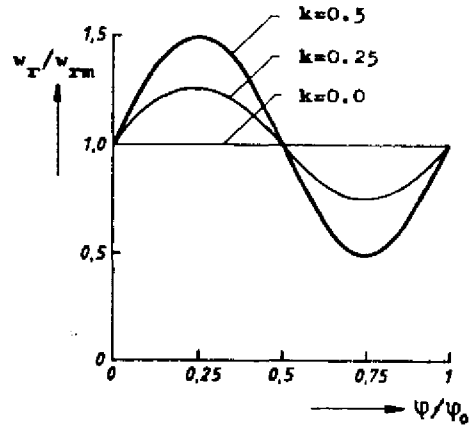


**Fig. 11** Radial velocity distribution chosen along a diffuser sector corresponding to a rotor channel angle

k will be set 0.0, 0.25 and 0.5 for the three cases respectively. For all these casses the velocity in the z-direction will be considered to be constant, which means, that there are no boundary layers at the entrance of the diffuser. The flow angle for the three casses will be assumed to be the same for the whole cross-section of the diffuser inlet ( $\beta_2 = 108^\circ$ ).
Figs.12 show the radial velocity development for k=0.5 along different radii and the vanishing of the velocity fluctuation.



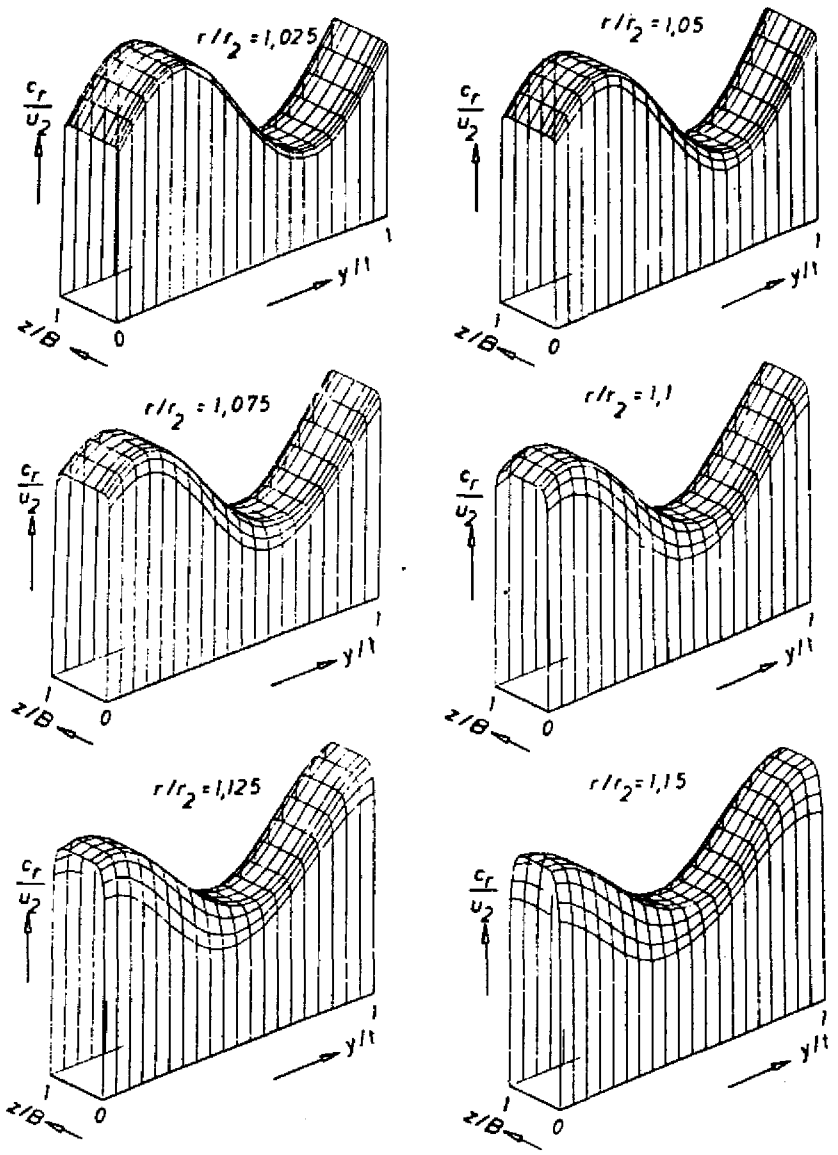


**Fig. 12a** Radial velocity development for different radii

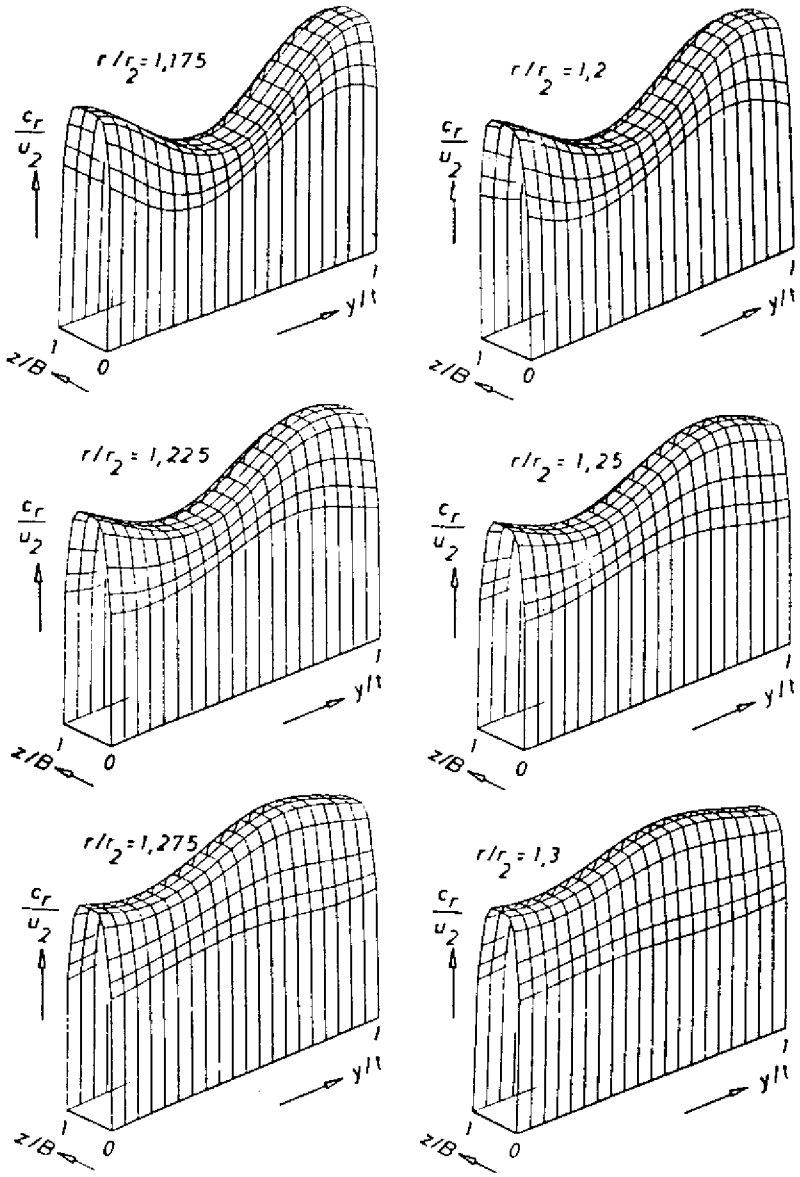


Fig. 12b Radial velocity development for different radii



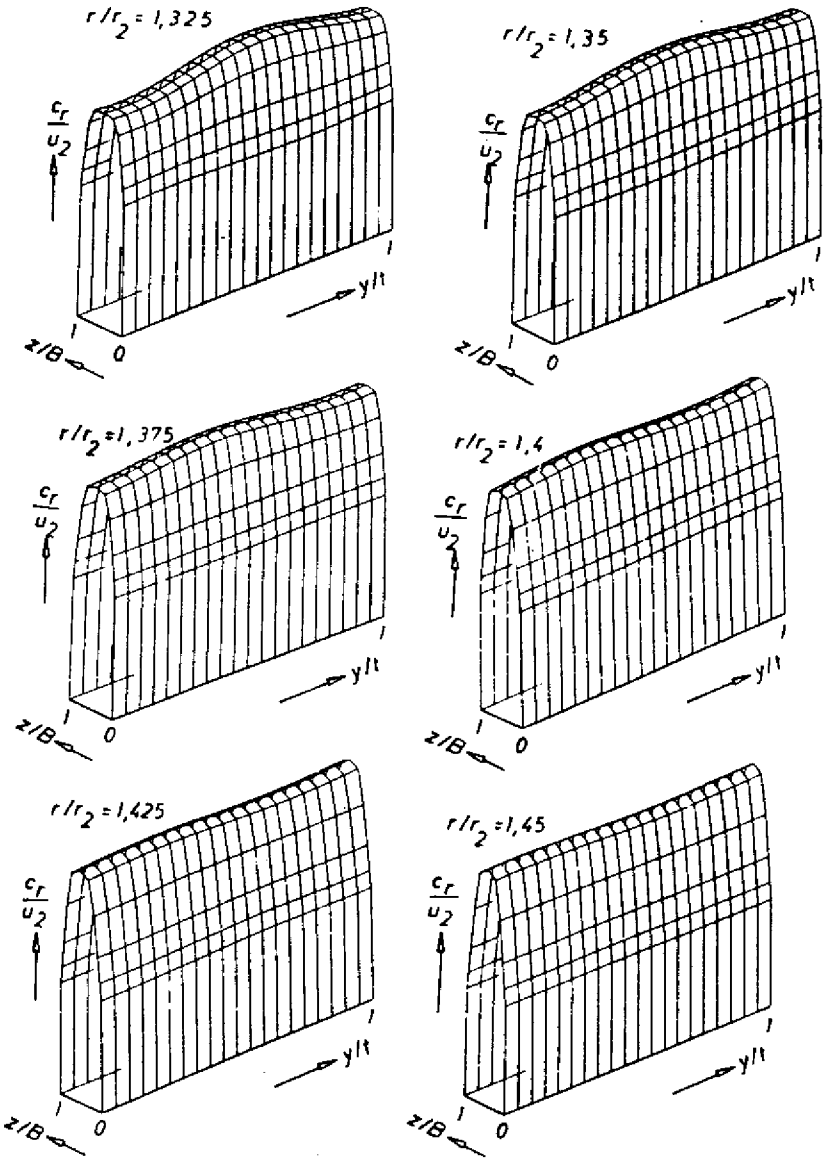


Fig. 12c Radial velocity development for different radii

The calculated diffuser efficiency $\eta_D$ for the three casses (k =0, 0.25 and 0.5 ) is ploted in Fig. 13.
The major part of the losses (drop in the efficiency) occurs in the mixing zone at the entrance of the diffuser. After that the gradient of all curves are almost the same. The distorted flow causes more losses than that caused by the uniform flow (k = 0). The decay of the wakes occur in relatively short radius ratio (here $R/R_2$ = 1.2) after the impeller. Even small distortion in the flow can produce fairly high losses at the entrance of the diffuser. The drop in the diffuser efficiency is found to be nonlinear with the distortion parameter k but almost hyperbolic.

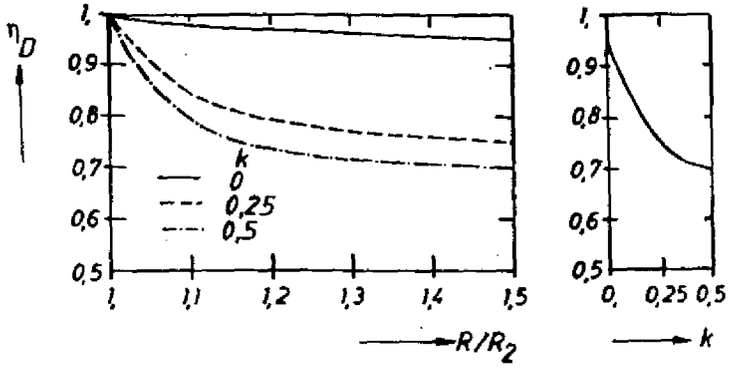


**Fig. 13** Diffuser efficiency for different distortion parameter k

## Conclusion

In this paper a procedure is presented to calculate the unsteady flow discharging from a radial compressor rotor in a vaneless diffuser. The parially parabolic method used in the calculation can be reguarded here as pure parabolic method, because the pressure field, which normally gives the elliptic effect, is estimated here parabolically assuming one dimensional flow conditions. For determinig the apparent viscosity all over the flow sections, a simple model based on Prandtl's assumptions is used.
The accuracy of the presented procedure is examined and a good agreement has been gained between the calculated and the measured values.
To study the effect of the unsymmetrical flow on the losses, hypothetical flow conditions having different distortion grades are calculated. It is stated that, even small flow distortion can produce fairly high losses in the zone of the diffuser entrance (mixing zone). The drop in diffuser efficiency is found to be hyperbolic with the distortion parameter k.



ACKNOWLEDGMENTS

The author would like to thank Professor Abdus Salam, the International Atomic Energy Agency and UNESCO for hospitality at the International Centre for Theoretical Physics, Trieste.

## Nomenculature

| | | |
|---|---|---|
| b | = | bridth of shear flow outside the boundary layers |
| B | = | diffuser width |
| c | = | absolute velocity |
| CD | = | continuity defect |
| DS | = | pressure side |
| k | = | distortion parameter |
| l | = | mixing length |
| $\dot{m}$ | = | mass rate of flow |
| N | = | revolution number |
| p | = | static pressure |
| $p_t$ | = | total pressure |
| $p_{tO}$ | = | atmospheric pressure |
| r | = | radius |
| R | = | radius |
| SS | = | suction side |
| t | = | blade period |
| u | = | circumferential velocity |
| $u_\tau$ | = | friction velocity |
| w | = | relative velocity |
| y | = | length in circumferential direction |
| z | = | axial direction |
| z | = | number of blades |
| $\beta_2$ | = | relative flow angle at impeller outlet |
| $\eta_D$ | = | diffuser efficiency |
| $\mu$ | = | dynamic viscosity |
| $\rho$ | = | density |



| | | |
|---|---|---|
| $\varphi$ | = | circumferential angle |
| $\varphi_o$ | = | channel angle |
| $\omega$ | = | angular velocity |

### Subscripts

| | |
|---|---|
| 2 | impeller exit (diffuser inlet) |
| l | laminar |
| max | maximum |
| min | minimum |
| r | radial component |
| t | turbulent |
| z | axial component |
| $\varphi$ | circumferential component |

### Superscripts

| | |
|---|---|
| * | not exactly calculated value |
| ' | correction part |
| - | mean value |

### References


[1] R.C. Dean,JR. and Senoo,Y., "Rotating Wakes in Vaneless Diffusers", TRANS.ASME, Journal of Basic Eng., Sept. 1960

[2] Eckardt,D., " Untersuchung der Strahl/Totwasser-Strömung hinter einem hochbelasteten Radialverdichterlaufrad ", Dissertation, RWTH Aachen, W. Germany, 1977

[3] Traupel,W., "Thermische Turbomaschinen", 1.Bd, Springer-Verlag, Berlin, Heidelberg, New York, 1977

[4] Johnston,J.P. and R.C. Dean,JR., " Losses in Vaneless Diffusers of Centrifugal Compressors and Pumps, Analysis, Experiment, and Design ",TRANS. ASME, Journal of Eng. for Power, Jan 1966

[5] M. Bassily Hanna," Berechnung der Ausgleichsvorgänge hinter einem Radialverdichterlaufrad ", Mitteil. Nr. 83-01 des Instituts für Strahlantriebe und Turboarbeitsmaschinen der RWTH Aachen, W. Germany, Sept. 1983

[6] Moore, J., and J.G. Moore, "A Calculation Procedure for Three-Dimensional, Viscous, Compressible Duct Flow " Part I and II, TRANS. ASME, JFE, 1979

[7] P. Lucking, " Numerische Berechnung der dreidimensionalen reibungsfreien und reibungbehafteten Strömung durch Turbomaschinen ", Dissertation, RWTH Aachen, W. Germany, 1982